$$\int \psi_A^0(Z=1,\ \vec{r}-\vec{R})\psi_D^0(Z=1,\ \vec{r})d\vec{r}\Big|^2, \quad (15)$$

which become for $\rho \geq 1.2\rho_0$:

$$\frac{\tau_{HL}}{\tau} = \frac{I}{I_{HL}} = \left| 1 - \sigma\rho + \frac{\sigma^2}{5}\,\frac{\rho^4+2\rho^3-3\rho^2-15\rho-15}{\rho^2+\rho+1} \right|^2 . \quad (16)$$

The maximum value of σ obtained by the variation principle is 0.15 and this occurs for $\rho_0 = 1.5$ ($R = 13.6$ Å) and $Z = 1$. For this case the ratios given in Eq. (16) are 0.55 and approach unity for larger values of ρ_0.

V. CONCLUSIONS

Summarizing, we have included configuration interaction in the quantum mechanics of the electronic states of donor-acceptor pairs and thus substantially improved the agreement between theory and experiment of the dependence of the radiative transition energy on donor-acceptor distance. A small revision in the sum of the ionization energies of separated donor and acceptor is probable. The possible origins of the remaining slight discrepancy in the R dependence are considered. The effect of configuration interaction on radiative lifetimes of pairs is evaluated and the theoretical lifetimes are found to be increased by as much as a factor of 2.

*Supported in part by a grant from the U. S. Army Research Office.

†Present address: Shepherd College, Shepherdstown, W. Va.

[1]F. E. Williams, J. Phys. Chem. Solids 12, 265 (1960); for a review see Phys. Status Solidi 25, 493 (1968).

[2]J. J. Hopfield, D. G. Thomas, and M. Gershenzon, Phys. Rev. Letters 10, 162 (1963).

[3]S. C. Wang, Phys. Rev. 31, 579 (1928).

[4]N. Rosen, Phys. Rev. 38, 2099 (1931).

[5]J. C. Shaffer and F. E. Williams, *Physics of Semiconductors* (Dunod, Paris, 1964), p. 811.

PHYSICAL REVIEW B VOLUME 6, NUMBER 10 15 NOVEMBER 1972

Magnetophonon Structure in the Longitudinal Magnetoresistance of Nonpolar Semiconductors

Robert L. Peterson

National Bureau of Standards, Quantum Electronics Division, Boulder, Colorado 80302

(Received 25 February 1972)

The magnetophonon effect in nonpolar nondegenerate semiconductors is investigated by solving the Boltzmann equation exactly in the Ohmic limit for combined optical- and acoustic-phonon scattering of carriers in parallel electric and magnetic fields. The solution is used in computing the longitudinal magnetoresistance at several temperatures and ratios of acoustic- to optical-phonon scattering. As this ratio increases from zero at intermediate temperatures, the Gurevich–Firsov (GF) resonance maxima are found to broaden and shift toward higher magnetic field, with pronounced minima developing at the resonance fields before the magnetophonon structure vanishes at large acoustic-phonon scattering. As the temperature increases, additional (pseudoresonance) minima develop between the GF extrema, and are comparable in amplitude to the latter when kT approximates the optical-phonon energy. At these temperatures the GF extrema are minima, even in the absence of elastic scattering. The results are compared with displaced-Maxwellian computations. The various effects are explained by physical arguments, which suggest that the same effects should occur for polar materials also.

I. INTRODUCTION

The magnetophonon effect is an oscillatory behavior of various transport properties of nondegenerate semiconductors, as a function of applied magnetic field, and is due to resonant interactions between the longitudinal-optical (LO) phonons of the material and the cyclotron motion of the charge carriers. The resonance magnetic fields are defined by

$$N\omega_c = \omega_0 , \quad (1)$$

where N is an integer, ω_0 is the angular frequency of the LO phonons at $k = 0$, and ω_c is the cyclotron frequency, given by $\omega_c = eB/m^*$, where B is the magnetic field, and m^* is the carrier effective mass. These resonances will here be referred to as the Gurevich–Firsov (GF) resonances, after the first workers in the field.[1,2]

Measurements of Ohmic longitudinal magnetore-

sistance (OLMR) in fairly pure nondegenerate *polar* semiconductors (Refs. 3 and 4 list most of such work) typically show minima at or near the resonance fields, although some quite polar materials[5–7] show extrema well displaced from the fields. The only published OLMR magnetophonon observation on a nonpolar material is that of Sokolov and Tsidil'kovskii,[8] who reported resonance minima in n-Ge. This, however, has not been confirmed by Eaves, Stradling, and Wood.[9]

The approximate theoretical analysis of Gurevich and Firsov on OLMR[2] was carried out for polar materials, and suggested that the extrema at the resonance fields should be maxima if LO-phonon scattering is dominant, and minima otherwise. However, the common observation of OLMR minima under circumstances for which LO-phonon scattering is dominant has contradicted this conclusion. Later studies[4,10] based on the displaced Maxwellian distribution function, taking into account the simultaneous action of several elastic scattering mechanisms in varying strengths in polar materials, did not resolve this question, but did show that strong carrier-carrier scattering prevents the development of GF resonance minima in OLMR.

Recently, however, it has been recognized that the magnetophonon analysis is considerably simpler in nonpolar materials. Kharus and Tsidil'kovskii[11] were able to conclude that there could be GF minima even in the absence of elastic scattering provided the temperature was high enough. My analysis, made independently and reported briefly[12] (Ref. 12 is hereafter referred to as I), confirmed this and showed that the GF minima can be well developed even at temperatures which are not particularly high ($kT \approx \frac{1}{2}\hbar\omega_0$). Thus the maxima-minima puzzle in OLMR can be considered at least partially resolved.

The emphasis of I, however, was upon a different phenomenon which was referred to as a "pseudoresonance" behavior. The purpose of the present paper is to elaborate upon the material presented in I, and to supply some additional results. It was shown there by general arguments that a new type of oscillatory behavior intermixed with the GF resonances should exist, with extrema lying at magnetic fields given by

$$\omega_c/\omega_0 = 2/(2n+1), \quad n = 0,\ 1,\ 2 \ldots \tag{2}$$

in contrast to the GF resonances described by Eq. (1). Computations showed that the pseudoresonance amplitudes could be comparable in magnitude to the GF amplitudes at the higher temperatures; i.e., $kT \approx \hbar\omega_0$.

In this paper, the solution to the Boltzmann equation, for combined LO- and acoustic-phonon scattering in nonpolar materials, is shown in the Ohmic longitudinal case. An expression for the OLMR is developed, which is particularly useful in computing. A physical picture of the mechanisms responsible for the various effects is also given. The simple model of the band structure—parabolic, isotropic, and centered at $k = 0$—is used, and the influence of Landau level collisional broadening is not included. Level broadening has been treated, e.g., by Dworin,[13] Nakayama,[14] and Barker,[15] for the transverse case, where it is essential for removing divergences at the GF resonances. Broadening effects should not be as important in the longitudinal case, since the amplitudes are already finite, but can be expected to become more significant with decreasing B and increasing T. The results of numerical computations are shown for several temperatures, and mixtures of elastic-inelastic scattering ranging from pure acoustic phonon, in which the results of Dubinskaya[16] are extended, to pure LO scattering. In several figures we show how the GF extrema and the pseudoresonances vary with temperature and elastic scattering, as determined by the Boltzmann equation. The results are compared with displaced Maxwellian computations in a few cases. From this comparison, the role of carrier-carrier scattering on the magnetophonon structure may be inferred.

II. THEORETICAL DEVELOPMENT

Ohmic mobility expressions for zero magnetic field, for combined LO- and acoustic-phonon scattering in nonpolar materials may be found, e.g., in Conwell,[17] and will not be repeated here. The Hamiltonian describing a carrier of momentum $\vec{p}$ and charge $-e$ with $e > 0$, interacting with the lattice, and in parallel electric and magnetic fields in the z direction, is, in the "Landau gauge,"

$$H = [\,p_x^2 + p_z^2 + (p_y + m^*\omega_c x)^2\,]/2m^* + H_L + \textstyle\sum_\alpha V_\alpha + eEz\ , \tag{3}$$

where H_L is the lattice Hamiltonian, and V_α describes the interaction between the carrier and phonons of type α.

The energy eigenvalues of the first term on the right-hand side in Eq. (3) are

$$\mathcal{E}_n(k_z) = \hbar^2 k_z^2/2m^* + \hbar\omega_c(n + \tfrac{1}{2})\ . \tag{4}$$

There is an N_y-fold energy degeneracy associated with the y direction. With

$$s = \hbar\omega_c/kT\ , \tag{5}$$

the equilibrium distribution function may be written

$$f_n^0(k_y, k_z) = N_y^{-1}(\beta\hbar^2/2\pi m^*)^{1/2}(1 - e^{-s}) \times \exp(-ns - \beta\hbar^2 k_z^2/2m^*)\ , \tag{6}$$

normalized such that

$$\sum_{k_y}\sum_{n=0}^{\infty}\int_{-\infty}^{\infty} dk_z f_n^0(k_y, k_z) = 1 . \tag{7}$$

The steady-state Boltzmann equation becomes

$$\frac{-eE}{\hbar}\frac{\partial f_n(k_y, k_z)}{\partial k_z} = \sum_{n'k_y'k_z'} [w(nk_y k_z, n'k_y' k_z') \times f_{n'}(k_y', k_z') - w(n'k_y' k_z', nk_y k_z) f_n(k_y, k_z)] . \tag{8}$$

The transition probabilities for either of the two phonon scattering processes are

$$w^{\alpha}(nk_y k_z, n'k_y' k_z') = \frac{2\pi}{\hbar}\sum_{\vec{q}} |J_{n'n}|^2 [B^{\alpha}(q)\delta_{k_y'-k_y, q_y} \times \delta_{k_z'-k_z, q_z}\delta_+ + A^{\alpha}(q)\delta_{k_y'-k_y, -q_y}\delta_{k_z'-k_z, -q_z}\delta_-] , \tag{9}$$

$$w^{\alpha}(n' k_y' k_z', nk_y k_z) = \frac{2\pi}{\hbar}\sum_{\vec{q}} |J_{n'n}|^2 [A^{\alpha}(q)\delta_{k_y'-k_y, q_y} \times \delta_{k_z'-k_z, q_z}\delta_+ + B^{\alpha}(q)\delta_{k_y'-k_y, -q_y}\delta_{k_z'-k_z, -q_z}\delta_-] , \tag{10}$$

where

$$\delta_{\pm} = \delta[\hbar^2(k_z^2 - k_z'^2)/2m^* + \hbar\omega_c(n - n') \pm \hbar\omega_{q,\alpha}] , \tag{11}$$

$$A^{\alpha}(q) = |\bar{q}_{\alpha}|^2 \bar{n}_{q,\alpha} , \tag{12}$$

$$B^{\alpha}(q) = |\bar{q}_{\alpha}|^2 (\bar{n}_{q,\alpha} + 1) . \tag{13}$$

The Planck factor at lattice temperature $T = 1/k\beta$ specifies the number of thermal phonons of type α in mode $\vec{q}$, of angular frequency $\omega_{q,\alpha}$:

$$\bar{n}_{q,\alpha} = (e^{\beta\hbar\omega_{q,\alpha}} - 1)^{-1} . \tag{14}$$

The usual assumptions of no dispersion for the LO modes ($\omega_q = \omega_0$), and linear dispersion for the longitudinal-acoustic modes ($\omega_q = qu_l$) are made. The coupling coefficients $|\bar{q}_{\alpha}|^2$ for the nonpolar optical-phonon and deformation-potential acoustic-phonon scattering are, respectively,

$$|\bar{q}_{\mathrm{op}}|^2 = E_{1\,\mathrm{op}}^2 \hbar\omega_0/2\Omega\rho u_l^2 , \tag{15}$$

$$|\bar{q}_{\mathrm{ac}}|^2 = E_1^2 \hbar q^2/2\Omega\rho u_l , \tag{16}$$

where Ω is the volume of the sample and ρ is its mass density; $E_{1\,\mathrm{op}}$ and E_1 are both deformation-potential parameters[17] with dimensions of energy.

In Eqs. (9) and (10), $J_{n'n}(q_x, k_y + q_y, k_y)$ is the matrix element of the carrier part of V_{α},

$$\langle n', k_y + q_y, k_z + q_z | e^{i\vec{q}\cdot\vec{r}} | n, k_y, k_z\rangle \equiv J_{n'n}(q_x, k_y + q_y, k_y) , \tag{17}$$

and can be expressed as an integral over harmonic oscillator wave functions.[4,18,19] However, with the usual assumptions of elasticity and equipartition for the acoustic phonons, and no dispersion for the LO phonons, one does not need to know the form of $J_{n'n}$, but can use the enormously simplifying result

$$\int_{-\infty}^{\infty}\int_{-\infty}^{\infty} dq_x dq_y |J_{n'n}|^2 = 2\pi m^*\omega_c/\hbar . \tag{18}$$

The left-hand side of Eq. (18) does not occur for the polar optical-phonon scattering, nor for impurity scattering, or acoustic-phonon scattering via the piezoelectric interaction.

Equation (8) is linearized in E by writing

$$f_n(k_y, k_z) = f_n^0(k_y, k_z) + f_n^1(k_y, k_z) , \tag{19}$$

where $f_n^1(k_y, k_z)$ is linear in E, odd in k_z, and independent of k_y. The "arrival" scattering term in Eq. (8) vanishes, leaving the "departure" term to define a relaxation time. The Boltzmann equation is solved for $f_n^1(k_y, k_z)$, and the mobility is calculated from

$$v_d \equiv -\mu_B E = (\hbar/m^*)\sum_{k_y, n}\int_{-\infty}^{\infty} dk_z k_z f_n^1(k_y, k_z) . \tag{20}$$

For either of the two mechanisms acting alone, one obtains

$$\mu_B^{\mathrm{ac}} = 3Ab\bar{n}_0\gamma(1 - e^{-s})G^{\mathrm{ac}}(s)/s , \tag{21}$$

$$\mu_B^{\mathrm{op}} = 6A(1 - e^{-s})G^{\mathrm{op}}(\gamma, s)/s , \tag{22}$$

where

$$\gamma = \hbar\omega_0/kT , \tag{23}$$

$$b = (E_{1\,\mathrm{op}}/E_1)^2 , \tag{24}$$

$$A = \frac{4e\hbar^4\rho u_l^2}{3E_{1\,\mathrm{op}}^2\bar{n}_0\hbar\omega_0}\left(\frac{2\pi}{m^{*5}kT}\right)^{1/2} , \tag{25}$$

$$G^{\mathrm{ac}}(s) = \sum_{n=0}^{\infty} e^{-ns}\int_0^{\infty}\frac{dz\, z^2 e^{-z^2}}{D_n^{\mathrm{ac}}(z^2, s)} , \tag{26}$$

$$G^{\mathrm{op}}(\gamma, s) = \sum_{n=0}^{\infty} e^{-ns}\int_0^{\infty}\frac{dz\, z^2 e^{-z^2}}{D_n^{\mathrm{op}}(z^2, \gamma, s)} , \tag{27}$$

$$D_n^{\mathrm{ac}}(z^2, s) = \sum_{n'}[z^2 - s(n' - n)]^{-1/2} , \tag{28}$$

$$D_n^{\mathrm{op}}(z^2, \gamma, s) = \sum_{n'}\{[z^2 + \gamma - s(n' - n)]^{-1/2} + e^{\gamma}[z^2 - \gamma - s(n' - n)]^{-1/2}\} . \tag{29}$$

In Eqs. (28) and (29), the terms $[\ ]^{-1/2}$ are zero if the radicands are less than zero.

The integrands in Eqs. (26) and (27) are discontinuous and difficult to work with numerically. Dubinskaya[16] considered the Ohmic longitudinal magnetoresistance for pure deformation-potential acoustic-phonon scattering, using expressions equivalent to Eqs. (21), (26), and (28), first given by Argyres,[19] and Gurevich and Firsov.[2] By rewriting $G^{\mathrm{ac}}(s)$ and using tables, Dubinskaya computed $\Delta\rho/\rho_0$ for $s > 0.6$ and showed that for $0.6 < s < 2$, the magnetoresistance is negative. It has been observed that $G^{\mathrm{ac}}(s)$ can be reexpressed in a yet simpler form, by transforming the range of integration in each interval for which the integrand is continuous, back to the interval 0–1, and collecting terms (see Appendix). Thus

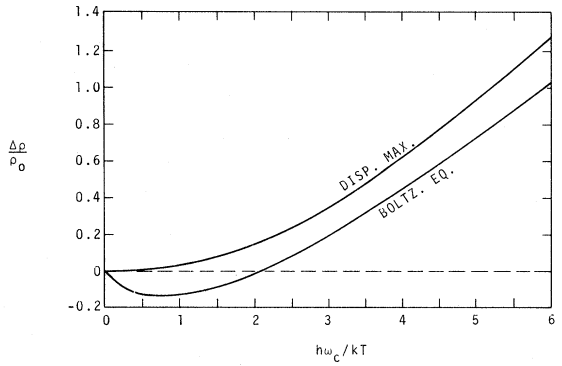

FIG. 1. Ohmic longitudinal magnetoresistance due to deformation-potential acoustic-phonon scattering, as calculated by the displaced Maxwellian and Boltzmann equation techniques.

$$G^{ac}(s)=\frac{s^2}{2}\int_0^1 dy\, e^{-sy}\sum_{n=0}^{\infty} e^{-ns} \times\left(\sum_{n'=0}^{n}(y+n')^{1/2}\Big/\sum_{n'=0}^{n}(y+n')^{-1/2}\right). \quad (30)$$

This form is simple to work with by computer, and Fig. 1 shows the resulting longitudinal magnetoresistance. Computations were carried down to $s=\frac{1}{8}$. The results coincide with those of Dubinskaya for $s>0.6$. Also shown in Fig. 1 are results computed with the displaced Maxwellian, using the assumptions of elastic collisions and equipartition, as with the Boltzmann equation. The displaced Maxwellian expressions are given in Ref. 4. No region of negative magnetoresistance occurs, the over-all magnetoresistance being rather uniformly higher. Comparison of the curves shows the effects of carrier-carrier scattering, implied by the displaced Maxwellian.

The nonpolar optical-phonon scattering term $G^{op}(\gamma, s)$ is not so easily transformed and computed. However, the same transformations and resummations as used with the acoustic-phonon term considerably simplify the computation (see Appendix). Thus, for the combined action of the optical and acoustic phonons, one obtains

$$\mu_B^c = 6A(1-e^{-s})\,G^c(\gamma, s)/s\ , \quad (31)$$

where

$$G^c(\gamma, s)=\tfrac{1}{2}s^2\sum_{n=0}^{\infty} e^{-ns}\int_0^1 dy\, e^{-sy} \times\sum_{n'=0}^{n}(y+n')^{1/2}/\zeta_n(y, s)\ , \quad (32)$$

$$\zeta_n(y, s)=C\sum_{n'=0}^{n}(y+n')^{-1/2}+\sum_{n'=-\infty}^{n}\left[(y+n'+\gamma/s)^{-1/2} + e^{\gamma}(y+n'-\gamma/s)^{-1/2}\right], \quad (33)$$

$$C=2/\gamma\bar{n}_0 b\ . \quad (34)$$

Here, C is the ratio of acoustic- to optical-phonon scattering, including thermal excitation of the respective phonons. The quantities $(y+n'\pm\gamma/s)^{-1/2}$ are defined to be zero for negative argument. The integrand of $G^c(\gamma, s)$ has at most two discontinuities in the interval 0–1, one from LO-phonon emissions (the term multiplied by e^{γ}) and one from LO-phonon absorptions. At the GF resonances [Eq. (1)], these discontinuities have moved to the boundaries of this interval. The two discontinuities merge at the center of the interval for the pseudoresonance values of B, specified by Eq. (2). These values may be determined by setting the LO radicands in Eq. (33) equal to zero at $y=\frac{1}{2}$, or more generally by the method in I.

One can understand the reason for the pseudoresonances in physical terms as follows. In I it was pointed out that the pseudoresonances occur when emission and absorption transitions ending at $k_z=0$ pair off, that is, when both have the same finite initial value of k_z. Figure 2 depicts the most important of such transitions at magnetic fields near the pseudoresonance field at $\omega_c=2\omega_0/3$. Absorptions a and b' always originate from the same k_z. Absorption a involves the lowest-energy carrier, and is a dominant transition, limiting the mobility. [This may be confirmed by inspecting the $n=0$ and $n=1$ terms of Eq. (32).] In spite of this, it actually plays only an indirect role in determining the amplitude of the pseudoresonance, contrary to a statement made in I. In fact, the interplay of b and b', as well as c and c', is responsible for the abrupt change in the behavior of the mobility. A "mobility-limiting" transition is used here to mean a transition for which carriers of higher energy play a relatively smaller role in determining the mobility. Emission processes are considerably more effective than absorption processes as mobility limiters. Below the pseudoresonance field

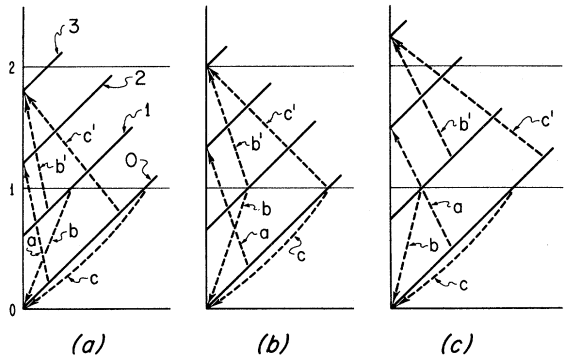

FIG. 2. Various LO transitions ending at $k_z=0$; (a), (b), (c), magnetic fields below, at, and above, respectively, the $\omega_c=2\omega_0/3$ pseudoresonance field. Carrier energy is plotted vertically, and $\hbar^2k_z^2/2m^*$ is plotted horizontally, both in units of $\hbar\omega_0$.

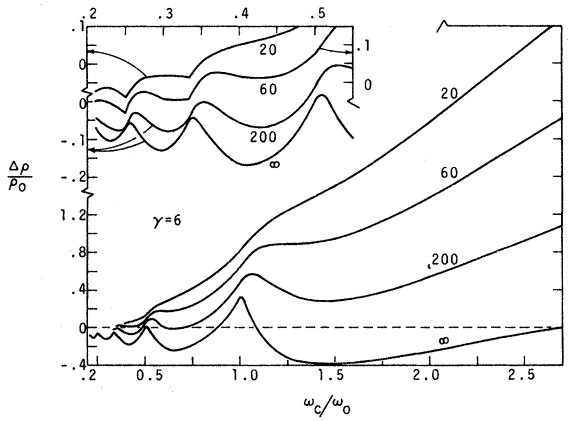

FIG. 3. Ohmic longitudinal magnetoresistance due to combined optical- and acoustic-phonon deformation-potential scattering at $T=\theta/6$, as calculated from the Boltzmann equation. Numbers on curves are values of $(E_{1\,op}/E_1)^2$. Several scales are used to separate the curves.

[Fig. 2(a)] the mobility is limited first by absorption a, and secondarily by absorptions b' and c'. As the field increases, these transitions are pushed back to the more energetic carriers, and the mobility is correspondingly increased. At the pseudoresonance field [Fig. 2(b)] emission transitions b and c occur for carriers with the same energy as those undergoing absorptions b' and c'. At higher fields [Fig. 2(c)] emissions b and c are the mobility limiters, and their carriers maintain the energy $\hbar\omega_0$ as the magnetic field increases further. It is the change of the mobility-limiting mechanism from absorption to emission at the pseudoresonance fields that produces the resistance minima.

In fact, the same mechanism is in part responsible for the minima which appear at the GF fields, a fact which has not apparently been realized earlier.[2,11] The appearance of new elastic transitions as B increases through the GF fields generally makes a larger contribution to the GF minima, however. That is, the horizontal transitions to $k_z\approx 0$ replace LO emissions as the limiters (except at the $N\approx 1$ resonance). Thus, increasing elastic scattering tends to enhance the GF minima for $N>1$, opposing the tendency for all extrema to be "washed out" by the monotonic elastic background. Horizontal transitions to $k_z=0$ do not critically affect the pseudoresonances, however, as can be seen from a diagram such as Fig. 2, and so the pseudoresonance amplitudes can be expected to vanish more quickly with elastic scattering than the $N>1$ GF resonances.

The temperature dependence of the pseudoresonance amplitudes should vary approximately as $e^{-\gamma}/(e^{\gamma}+1)\approx e^{-2\gamma}$, which is the condition for the existence of the absorption processes b' and c' at the pseudoresonance field of Fig. 2. When the temperature is high enough to allow these processes, the emission processes b and c are also allowed. The GF minima would go principally as $e^{-\gamma}$ due to the single absorption process from near the bottom of the band. Landau level broadening will, of course, contribute additional temperature dependence, which should be more important at the lower magnetic fields.

III. NUMERICAL ANALYSIS AND DISCUSSION

The Ohmic longitudinal magnetoresistance is calculated as

$$\Delta\rho/\rho_0=\mu_0/\mu_B-1 \tag{35}$$

since changes in carrier concentration with B are neglected. In Figs. 3–6 the OLMR is shown for several lattice temperatures, and ratios b ranging from pure nonpolar optical-phonon scattering to predominantly acoustic-phonon scattering.

At the low temperature ($\gamma=6$) of Fig. 3, the curve for pure LO scattering shows fairly sharp GF maxima displaced slightly to the high-field side of the resonance fields, in agreement with the analysis of Bryksin[20] on polar materials, and of Kharus and Tsidil'kovskii[11] in the nonpolar case. As the amount of acoustic-phonon scattering increases, the maxima broaden and shift toward higher fields, while GF minima develop right at the resonance fields, appearing first and being most prominent at the low fields. Collisional broadening of the Landau levels should act against this trend. Finally, no pseudoresonances are in evidence at this low temperature.

For the higher temperature ($\gamma=3$) of Fig. 4, the

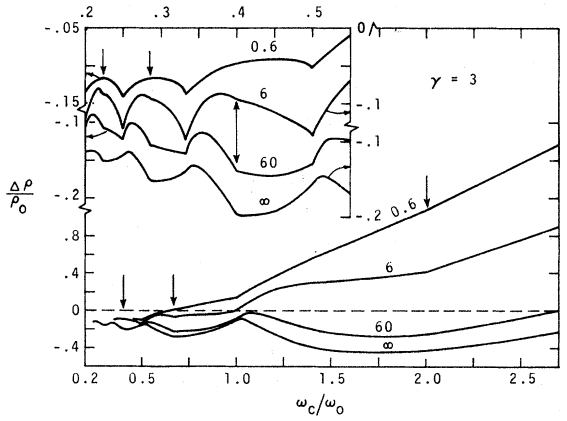

FIG. 4. Ohmic longitudinal magnetoresistance due to combined optical- and acoustic-phonon deformation-potential scattering at $T=\theta/3$, as calculated from the Boltzmann equation. Numbers on curves are values of $(E_{1\,op}/E_1)^2$. Arrows show the pseudoresonance positions. Several scales are used to separate the curves.

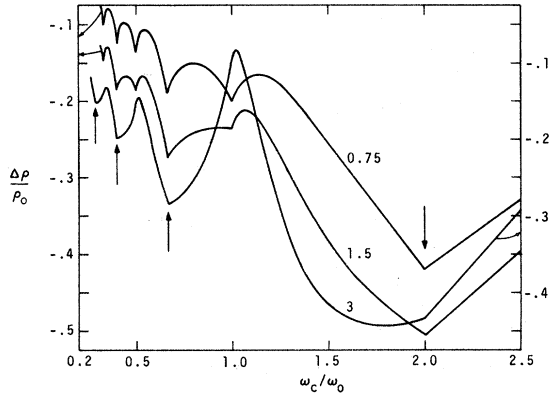

FIG. 5. Ohmic longitudinal magnetoresistance for nonpolar LO scattering only, as calculated from the Boltzmann equation. Numbers on curves are values of $\gamma=\theta/T$. Arrows show the pseudoresonance positions. Two scales are used for clarity.

pure LO curves show GF maxima shifted toward higher fields and less pronounced than at the lower temperature. The same trends in the GF resonances occur as in Fig. 3. Now, however, the pseudoresonances (marked by arrows in the figure) have developed to a small degree. To be noted is the fact that with increasing elastic scattering, the pseudoresonance amplitudes, which are always minima, decrease, whereas the GF minima first increase, then decrease as acoustic-phonon processes become completely dominant. The $b=0.6$ curve in Fig. 4 shows that the pseudoresonances have vanished while the GF minima are still prominent.

Figure 5 shows the changing magnetophonon structure with temperature for pure LO scattering. The $\gamma=3$ curve shows GF maxima and fairly well-developed pseudoresonance minima. Notice the broad minimum to the low-field side of the $\omega_c=2\omega_0$ pseudoresonance. This is the minimum discussed by Bryksin,[20] and should not be confused with the pseudoresonance. As the temperature is increased to $\gamma=1.5$ and 0.75, minima develop at the GF resonances. We emphasize that this occurs in the absence of elastic scattering, and shows that the reasoning of Gurevich and Firsov[2] concerning the importance of elastic processes in producing the minima, should not be understood as requiring that elastic processes are necessary for the achievement of the minima.

That elastic processes that do assist in forming OLMR GF minima can be seen by comparing with Fig. 6 ($b=6$). Also, one sees that the pseudoresonance amplitudes diminish with increasing elastic scattering.

The most important feature to be noted with regard to the pseudoresonances, however, is that at the higher temperatures they are generally as prominent as the GF resonances, and should be observable.

Minima at the pseudoresonance positions have indeed been observed, appearing only at high temperatures[3,5,21-25] ($\gamma\approx1$) or under hot-electron conditions.[26] The "extra" structure is usually comparable in magnitude to the GF structure at the higher temperatures, but has a temperature dependence which is quite different.[3,24] The extra structure also is smaller when elastic scattering is known to be stronger.[3] The pseudoresonance effect has each of these features, as seen in Figs. 3–6.

The observed extra structure has earlier been explained[3,24] as due to 2-LO processes, which have not been defined further apart from the statements that such processes should have a temperature dependence $e^{-2\gamma}$, a resonance condition $N\omega_c=2\omega_0$, $N=1, 2, \ldots$, and should be weakened by competition from elastic scattering. These features are characteristic of second-order (i.e., second Born approximation) LO processes.[27] A still earlier postulate invoked spin-flip transitions, but this explanation has now generally been abandoned.[3,24,26] Notice that the second-order resonance fields coincide with the fields at which the GF resonances and the pseudoresonances together occur. Both the GF resonances and pseudoresonances, of course, occur in first order. The second-order processes thus mimic the pseudoresonance behavior to a certain extent. No theoretical analysis is available at present for an accurate comparison. However, the success of the first-order calculations in providing a qualitatively correct description of the magnetophonon effect is a strong indication of the relative smallness of the second-order transition probabilities.

Some workers[26,28,29] have used the technique of

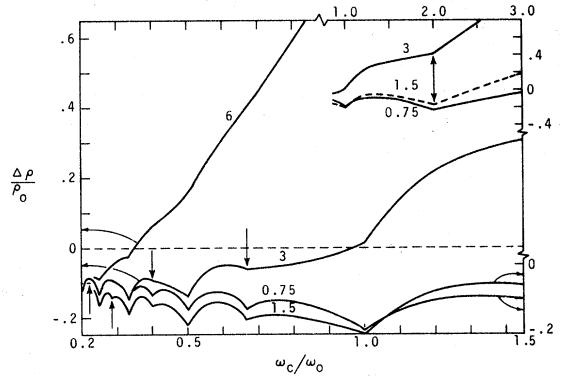

FIG. 6. Ohmic longitudinal magnetoresistance due to combined optical- and acoustic-phonon deformation-potential scattering at $(E_{1\,op}/E_1)^2=6$, as calculated from the Boltzmann equation. Numbers on curves are values of $\gamma=\theta/T$. Arrows show the pseudoresonance positions. Several scales are used to separate the curves.

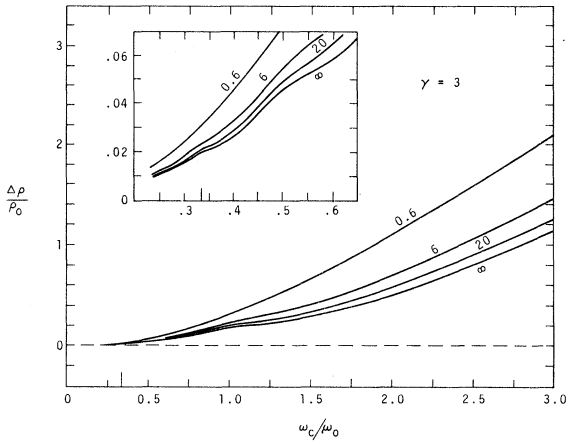

FIG. 7. Ohmic longitudinal magnetoresistance due to combined optical- and acoustic-phonon deformation-potential scattering at $T=\theta/3$, as calculated with the displaced Maxwellian distribution function. Numbers on curves are values of $(E_{1\,op}/E_1)^2$. Inset shows low-field region on an expanded scale.

applying non-Ohmic electric fields at very low temperatures to bring out structure which is otherwise unobservable. In addition to structure which can be identified as the GF resonances, other structure is also usually seen in the longitudinal configuration. Some of this consists of minima lying at the pseudoresonance positions[26,28]; no attempt was made to explain these minima. The pseudoresonance effect is possibly the correct explanation. The finite longitudinal electric field necessary to bring out the magnetophonon structure at very low temperature may also assist in bringing the carriers to values of k_z necessary for the existence of the pseudoresonance effect. This same idea may also be the explanation of why even in the Ohmic regime the pseudoresonance structure is seen more readily in the longitudinal configuration than the transverse, since in the latter the electric field does not assist in bringing the carriers to finite k_z.

Figure 7 shows a few results of displaced Maxwellian computations. Theoretical details may be found in Refs. 4 and 18. As is seen, the GF resonance extrema for pure optical-phonon scattering are maxima, but are much broader than as calculated by the Boltzmann equation. This is to be expected because of the carrier-carrier scattering implied by the displaced Maxwellian distribution function. With admixture of acoustic phonons, GF minima do not develop, as was also found for polar materials.[4] The maxima simply decrease in amplitude and become broader. Finally, the pseudoresonances are not present in the displaced Maxwellian description. This may be seen analytically[4,18] as well as in Fig. 7. Again, this is because of the carrier-carrier scattering, and is consistent with the trend seen in Figs. 3–6, in which the pseudoresonance amplitudes decrease monotonically with increasing elastic scattering.

In conclusion, although there is little magnetophonon data on nonpolar semiconductors, the Boltzmann equation analysis given here for nonpolar materials yields the over-all magnetophonon behavior generally observed in rather pure polar materials. The extra structure observed experimentally at the higher temperatures is probably the pseudoresonance effect. This is the natural interpretation; the effect is a first-order process, and our computations have shown that the pseudoresonance amplitudes can be as prominent as the GF amplitudes at the higher temperatures, and have qualitatively the correct elastic scattering and temperature dependence. Any other explanation has the twofold burden of justifying a proposed extra mechanism and showing why the pseudoresonances should not be significant.

ACKNOWLEDGMENT

I wish to thank R. A. Stradling for useful discussions which have led to my clearer understanding of the physical picture underlying the pseudoresonance effect.

APPENDIX

This Appendix will show the transformation and resummation technique used in obtaining Eqs. (30) and (32).

From Eq. (8) and (20), one may write the longitudinal mobility as

$$\mu_B = \frac{-e}{m^*} \sum_{n,k_y} \int_{-\infty}^{\infty} dk_z\, k_z \tau_n(k_z)\, \frac{\partial f_n^0(k_y,k_z)}{\partial k_z}\,, \tag{A1}$$

where $1/\tau_n(k_z)$ is a sum over the LO- and acoustic-phonon transition probabilities. Performing the necessary operations leads to Eq. (31), in which

$$G^c(\gamma,s) = \sum_{n=0}^{\infty} e^{-ns} \int_0^{\infty} dz\, z^2 e^{-z^2} / [C D_n^{ac}(z^2,s) + D_n^{op}(z^s,\gamma,s)]\,, \tag{A2}$$

where $z^2 = \hbar^2 k_z^2/2m^*kT$. Substituting $y = z^2/s$, consider the quantity

$$F(\gamma,s) \equiv 2G^c(\gamma,s)/s^2 = \sum_{n=0}^{\infty} \int_0^{\infty} dy\, y^{1/2}\, T(y+n)\,, \tag{A3}$$

where

$$T(y+n) = e^{-s(y+n)} \Big/ \sum_{n'=0}^{\infty} [C(y+n-n')^{-1/2} + (y+n-n'+\gamma/s)^{-1/2} + e^{\gamma}(y+n-n'-\gamma/s)^{-1/2}]\,. \tag{A4}$$

All quantities $x^{-1/2}$ are defined to be zero for $x \le 0$. The following manipulations hold regardless

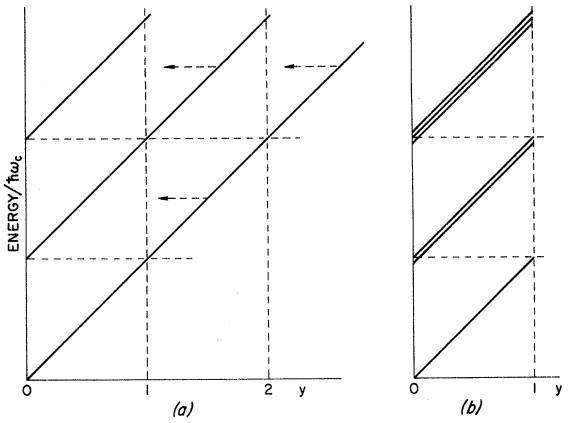

FIG. 8. Illustration of the effect of the transformation discussed in Appendix. Carrier energy is plotted vertically, and $\hbar^2k_z^2/2m^*$ is plotted horizontally, both in units of $\hbar\omega_c$.

of where the zeros of $T(y+n)$ lie; however, the motivation is to remove the zeros associated with the acoustic term (the term multiplied by C). Write

$$F(\gamma, s)=\left(\int_0^1+\int_1^2+\cdots\right)dy\, y^{1/2}T(y)$$
$$+\left(\int_0^1+\int_1^2+\cdots\right)dy\, y^{1/2}T(y+1)+\cdots . \quad \text{(A5)}$$

Transform each $\int_m^{m+1}$ back to $\int_0^1$, and collect terms common to $T(y+n)$:

$$F(\gamma, s)=\int_0^1 dy\, y^{1/2}\,T(y)+\int_0^1 dy\, T(y+1)$$
$$\times[y^{1/2}+(y+1)^{1/2}]+\cdots+\int_0^1 dy\, T(y+n)$$
$$\times\sum_{n'=0}^{n}(y+n')^{1/2}+\cdots$$
$$=\sum_{n=0}^{\infty}\int_0^1 dy\, T(y+n)\sum_{n'=0}^{n}(y+n')^{1/2} . \quad \text{(A6)}$$

Equation (32) follows at once.

The transformation has a simple physical interpretation. The original variable y is the carrier kinetic energy measured in units of $\hbar\omega_c$. The translations and collecting of terms is equivalent to making cuts on the y axis at the points 1, 2, ... [see Fig. 8(a)], and sliding each strip to the left to coincide with the first strip [Fig. 8(b)]. Then, e.g., transitions c and c' in Fig. 2 will, respectively, overlap transitions b and b'. The effect of the transformation is to remove the energy degeneracy of the different Landau levels, in the sense that each pair of values (y, n) in Eqs. (A6) or (32) specifies a distinct carrier energy.

[1]V. L. Gurevich and Yu. A. Firsov, Zh. Eksperim. i Teor. Fiz. 40, 198 (1961) [Sov. Phys. JETP 13, 137 (1961)].

[2]V. L. Gurevich and Yu. A. Firsov, Zh. Eksperim. i Teor. Fiz. 47, 734 (1964) [Sov. Phys. JETP 20, 489 (1965)].

[3]R. A. Stradling and R. A. Wood, J. Phys. C 1, 1711 (1968).

[4]R. L. Peterson, Phys. Rev. B 5, 3994 (1972); NBS Tech. Note 614 (U.S. GPO, Washington, D. C., 1972).

[5]L. Eaves, R. A. Stradling, S. Askenazy, J. Leotin, J. C. Portal, and J. P. Ulmet, J. Phys. C 4, L42 (1971).

[6]A. L. Mears, R. A. Stradling, and E. K. Inall, J. Phys. C 1, 821 (1968).

[7]L. Eaves, R. A. Stradling, S. Askenazy, G. Carrere, J. Leotin, J. C. Portal, and J. P. Ulmet, J. Phys. C 5, L19 (1972).

[8]V. I. Sokolov and I. M. Tsidil'kovskii, Fiz. Tekh. Poluprov. 1, 835 (1967) [Sov. Phys. Semicond. 1, 695 (1967)].

[9]L. Eaves, R. A. Stradling, and R. A. Wood, in *Proceedings of the Tenth International Conference of Semiconductors, Cambridge* (U.S. AEC, Washington, D. C., 1970), p. 816.

[10]R. L. Peterson, B. Magnusson, and P. Weissglas, Phys. Status Solidi 46, 729 (1971).

[11]G. I. Kharus and I. M. Tsidil'kovskii, Fiz. Tekh. Poluprov. 5, 603 (1971) [Sov. Phys. Semicond. 5, 534 (1971)].

[12]R. L. Peterson, Phys. Rev. Letters 28, 431 (1972).

[13]L. Dworin, Phys. Rev. 140, A1689 (1965).

[14]M. Nakayama, J. Phys. Soc. Japan 27, 636 (1969).

[15]J. R. Barker, Phys. Letters 33A, 516 (1970).

[16]L. S. Dubinskaya, Fiz. Tverd. Tela 7, 2821 (1965) [Sov. Phys. Solid State 7, 2280 (1966)].

[17]E. M. Conwell, in *Solid State Physics*, edited by F. Seitz, D. Turnbull, and H. Ehrenreich (Academic, New York, 1967), Suppl. 9, p. 167.

[18]R. L. Peterson, Phys. Rev. B 2, 4135 (1970).

[19]P. N. Argyres, J. Phys. Chem. Solids 4, 19 (1958).

[20]V. V. Bryksin, Fiz. Tverd. Tela 9, 232 (1967) [Sov. Phys. Solid State 9, 171 (1967)].

[21]I. M. Tsidil'kovskii, M. M. Aksel'rod, and V. I. Sokolov, Fiz. Tverd. Tela 7, 316 (1965) [Sov. Phys. Solid State 7, 253 (1965)].

[22]D. V. Mashovets, R. V. Parfen'ev, and S. S. Shalyt, Zh. Eksperim. i Teor. Fiz. Pis'ma v Redaktsiyu 1, 2 (1965) [Sov. Phys. JETP Letters 1, 77 (1965)].

[23]I. M. Tsidil'kovskii and M. M. Aksel'rod, J. Phys. Soc. Japan, Suppl. 21, 363 (1966).

[24]M. M. Aksel'rod and I. M. Tsidil'kovskii, Zh. Eksperim. i Teor. Fiz. Pis'ma v Redaktsiyu 9, 622 (1969) [Sov. Phys. JETP Letters 9, 381 (1969)].

[25]R. A. Stradling and R. A. Wood, J. Phys. C 3, L94 (1970).

[26]R. A. Stradling and R. A. Wood, J. Phys. C 3, 2425 (1970), Fig. 1.

[27]R. A. Stradling informs me that by "2-LO", he had in mind two absorption processes, not necessarily second Born approximation, such as b and b' in Fig. 2(b) with the direction of b reversed. Inspection of Eqs. (32) and (33) shows, however, that absorptions beginning at $k_z=0$ and ending at finite k_z play no essential role in developing the pseudoresonances.

[28]R. A. Stradling, L. Eaves, R. A. Hoult, A. L. Mears, and R. A. Wood, in Ref. 9, p. 369.
[29]M. M. Aksel'rod, V. F. Lugovykh, R. V. Pomortsev, and I. M. Tsidil'kovskii, Fiz. Tverd. Tela 11, 113 (1969) [Sov. Phys. Solid State 11, 81 (1969)].

PHYSICAL REVIEW B VOLUME 6, NUMBER 10 15 NOVEMBER 1972

Calculations of 2p-Exciton States in Semiconductors with Degenerate Bands*

N. O. Lipari†
University of Illinois, Urbana, Illinois and Xerox Corporation, Rochester, New York

and

A. Baldereschi
Bell Telephone Laboratories, Murray Hill, New Jersey 07974
(Received 26 May 1972)

Using a method previously introduced to treat s states, we analyze the 2p-excited states of direct excitons in semiconductors. The splitting of the four 2p levels, due to the degeneracy of the valence bands, are given by simple analytical expressions. The symmetry of these levels are discussed for the zinc-blende, diamond, and NaCl structures. Results are given for all semiconductors for which the valence-band parameters are known. Since the actual experimental situation is poor, suggestions are made as to which substances should be investigated in order to appreciate these splittings.

I. INTRODUCTION

Very recently, two-photon spectroscopy has gained increasing importance as a powerful method of studying electronic properties of solids.[1,2] Two-quantum absorption is a nonlinear optical phenomenon in which two quanta are simultaneously absorbed in an electronic or excitonic transition. Since the selection rules for two-photon transitions[3,4] are very different from those appropriate to one-photon transition,[5] the two methods are complementary. Moreover, since more state symmetries are observable in two-quantum absorption, one expects that more information concerning energy levels in solids can be obtained from two-quantum absorption than from single-quantum absorption. For excitons, the different selection rules involved in the two-quantum experiments[3,4] allow the observation of p states forbidden in the one-photon case. It is therefore evident that an accurate knowledge of these states is necessary to correctly interpret the results of the experimental analysis. Because of the anisotropy and the degeneracy of the valence bands[6] in all cubic semiconductors one cannot apply the simple hydrogenic model for the determination of these states; further, such degeneracy produces a splitting of the p states[1] which is clearly neglected if one uses the simple model.

In a previous set of papers,[7-9] we have set forth a method which solves the exciton problem in the case of degenerate bands, and we have applied it to treat the exciton ground state and the excited s-like states. In this paper we extend the method to treat the p-like excited states. We obtain very simple analytical expressions for the splitting of the various 2p states. Section II is a short analysis of the symmetry of the various states. In Sec. III we review briefly the general formulation of the problem and the method of solution, and in Sec. IV we apply the method to treat the 2p states. In Sec. V we discuss and summarize the results of the present investigation.

II. GROUP-THEORETICAL ANALYSIS

We now briefly describe the symmetry[10] of the p states in the diamond, zinc-blende, and NaCl structures. The exciton wave function can be written[11]

$$\psi(\vec{r}_e, \vec{r}_h) = \sum_i \chi^{(i)}(\vec{r}_e - \vec{r}_h)\,\phi_h^{(i)}(\vec{r}_h)\,\phi_e(\vec{r}_e)\,, \qquad (1)$$

where ϕ_e and $\phi_h^{(i)}$ are the Bloch functions for the electron and the hole, respectively, χ is the envelope function which describes the relative electron-hole motion, and i runs over the degenerate valence-band states. The symmetry of the exciton wave function is determined by the direct product of the irreducible representations for the envelope, hole, and electron wave functions.

For diamond crystals, the point group is O_h. The symmetry of the degenerate valence band at $\vec{k}=0$ is Γ_8^+ and the conduction-band minimum is Γ_2^- (Γ_6^- double-group notation). For the p states, in which we are interested, the envelope function has Γ_{15} symmetry and therefore we have